Coherent eta photoproduction on the deuteron in the S_{11} resonance region

E. Breitmoser and H. Arenhövel

Institut für Kernphysik, Johannes Gutenberg-Universität, D-55099 Mainz, Germany

Abstract

Coherent eta photoproduction on the deuteron is studied in the S_{11} resonance region neglecting eta rescattering and two-body processes. For the elementary reaction on the nucleon, we have considered the dominant $S_{11}(1535)$ resonance and as background the nucleon pole terms as well as ρ and ω meson exchange. We have studied the influence of different choices for the neutron resonance amplitude, different prescriptions for fixing the invariant mass of the resonance amplitude and different methods for deriving the elementary production amplitude for an arbitrary reference frame.

I. INTRODUCTION

In recent years, photo- and electroproduction of η mesons on nucleons and nuclei have been studied intensively [1,2,3]. This renewed interest has been triggered primarily by the significant improvement on the quality of experimental data obtained with the new generation of high-duty cycle electron accelerators like, e.g., ELSA in Bonn and MAMI in Mainz [4,5,6]. The special interest in the electromagnetic production of η mesons on the nucleon is based on the fact that, being an isoscalar meson, it constitutes a selective filter for isospin $I = \frac{1}{2}$ nucleon resonances N^*. Furthermore, the e.m. η production is dominated by the intermediate excitation of the $S_{11}(1535)$ resonance. Thus this reaction is an ideal

tool for investigating the characteristic features of this resonance, which usually is difficult to separate from the other resonances because of their large widths. For example, one can study its electromagnetic transition multipoles and its decay channels, thus providing a good test for hadron models.

Eta photoproduction on the deuteron is of particular interest since first it allows to study this reaction on a bound nucleon in the simplest nuclear environment, and second, it provides important information on this reaction on the neutron. With respect to the latter case, the deuteron is considered as a neutron target assuming that binding effects can be neglected. The first data for coherent η photoproduction on the deuteron were obtained almost thirty years ago by Anderson and Prepost [7]. Their results for the weighting of isoscalar and isovector amplitude of the $S_{11}(1535)$ resonance were at variance with quark model predictions and data analysis for pion photo production on the nucleon in the region of the S_{11} resonance. Only with a large isovector amplitude, the theory could explain the data assuming the validity of the impulse approximation [8]. Other explanations were proposed by Hoshi et al. [9] by invoking a dominance of η rescattering on the other nucleon or a large influence of the $P_{11}(1440)$ resonance. The latter seems to be ruled out at present. Furthermore, their treatment of rescattering is very approximate and a more recent evaluation of rescattering effects, although still approximate, gave a much smaller effect [10]. Therefore, improved calculations are urgently needed. Very recently, rescattering has been considered in [11] in the near threshold region showing only a small effect. It is clear that new data will offer the chance to investigate this problem in greater detail. With respect to new experimental data, only upper limits exist at present for the reaction on the deuteron [12,13] which, however, are already at variance with the old data.

The aim of the present work is to initiate a systematic study of the $d(\gamma, \pi^0)d$ reaction on the deuteron from threshold through the S_{11} resonance. As a first step, we will restrict ourselves to the plane wave impulse approximation (PWIA) in order to study details of the elementary reaction amplitude with respect to the yet unknown neutron properties and to study different ways of implementing the elementary amplitude in a bound system.

Among the phenomenological models describing existing data for the elementary process on the proton for energies below 1 GeV in a satisfactory manner, there are the isobar model [14], the coupled channel model [15] and the effective Lagrangian approach [16,17,18]. We have chosen the Langrangian approach of [16,17] because the resonance and background terms are treated on the same level and the number of unknown parameters is much less than that for the two other models. Near threshold the resonances $P_{11}(1440)$, $D_{13}(1520)$ and $S_{11}(1535)$ are likely to contribute. Although the $P_{11}(1440)$ is below the threshold, it can influence the reaction because of its large width. Little is known on the decay widths of the resonances $P_{11}(1440)$ and $D_{13}(1520)$ to ηN and they are not listed in [19]. In [20], the branching ratio of the $D_{13}(1520)$ into this channel is listed to be 0.1%. Furthermore, the experiment of Krusche et al. [5] did not give any evidence for the influence of the $P_{11}(1440)$, whereas the $D_{13}(1520)$ was seen for the first time. Nevertheless, it was shown that the influence of the $D_{13}(1520)$ to the total cross section was negligible. For these reasons, it is legitimate to consider in the present study only the dominant S_{11} resonance. In addition we include background terms such as nucleon pole terms and the exchange of the vector mesons ρ and ω. Apart from the resonance, also the strength and nature (pseudoscalar or pseudovector) of the ηNN-coupling is widely unknown.

When implementing the elementary reaction amplitude into the deuteron, one has to face several problems which are analogous to coherent π photoproduction on the deuteron. First of all, the energy of the struck nucleon on which the reaction takes place is not well defined in a bound nonrelativistic system. Consequently, the invariant mass of the γN subsystem of the elementary reaction, on which the elementary t-matrix depends, is not well defined. In particular, the invariant mass determines the decay width of the resonance to which the resulting cross section is very sensitive. Secondly, the elementary reaction amplitude, which usually is given in the γN c.m. frame, has to be transformed to an arbitrary reference frame. This may be done either by a Lorentz boost of all four momenta on which the elementary process depends or by calculating the t-matrix with respect to an arbitrary frame right from the beginning. The last method is more general because one does not loose any terms which

vanish in the γN c.m. frame. But in both cases one faces again the problem of assigning an energy to the bound nucleon. We will compare both methods for the contributions of vector meson exchange in order to check to what extent the differences matter.

The paper is organized as follows: In the next section we present the model for the elementary reaction, and fix all parameters for the process on the proton. Then we discuss in Sect. III the theoretical changes that have to be considered for the process on the deuteron. In Sect. IV we present our results and compare them with existing experimental data and other theoretical calculations. Finally, we give a brief summary and an outlook. Some calculational details are collected in an appendix.

II. THE ELEMENTARY PROCESS $\gamma + N \to \eta + N$

In this section, we will briefly review the elementary reaction in order to introduce the model and to fix as many model parameters as possible for the implementation of the process into the deuteron. The Mandelstam variables of the reaction $\gamma(k) + N(p) \to \eta(q) + N(p')$ are defined as usual

$$s = (k_\mu + p_\mu)^2 = (q_\mu + p'_\mu)^2, \tag{1}$$

$$t = (k_\mu - q_\mu)^2 = (p_\mu - p'_\mu)^2, \tag{2}$$

$$u = (k_\mu - p'_\mu)^2 = (q_\mu - p_\mu)^2, \tag{3}$$

where p_μ (p'_μ) denotes the four momentum of the incoming (outgoing) nucleon, k_μ and q_μ the momenta of photon and eta meson, respectively. The energies of the participating particles are given by

$$k_0 = |\vec{k}|, \tag{4}$$

$$\omega_q = \sqrt{m_\eta^2 + \vec{q}^{\,2}}, \tag{5}$$

$$E_{p^{(\prime)}} = \sqrt{M^2 + \vec{p}^{\,(\prime)\,2}}. \tag{6}$$

The invariant mass of the γN system is given as function of the photon lab energy E_γ^{Lab} by

$$W_{\gamma N} = \sqrt{s} = \sqrt{M^2 + 2E_\gamma^{Lab} M} \,, \tag{7}$$

and the absolute values of the three momenta in the c.m. system by

$$k = \frac{s - M^2}{2\sqrt{s}} \,, \tag{8}$$

$$q = \frac{1}{2\sqrt{s}} \sqrt{[s - (M + m_\eta)^2][s - (M - m_\eta)^2]} \,. \tag{9}$$

Nucleon and eta masses are denoted by M and m_η, respectively. In the c.m. system, the unpolarized differential cross section is given by

$$\frac{d\sigma}{d\Omega_\eta^{c.m.}} = \frac{1}{6} \frac{1}{16\pi^2} \frac{q}{k} \frac{E_k E_q}{W_{\gamma N}^2} \sum_{m'm\mu} |\tau_{m'm\mu}(W_{\gamma N}, \theta)|^2 \,, \tag{10}$$

where $\tau_{m'm\mu}$ denotes the t-matrix element for initial and final nucleon spin projections m and m', respectively, and photon polarization μ

$$\tau_{m'm\mu}(W_{\gamma N}, \theta) = \langle m'|t_{\gamma\eta}(W_{\gamma N})|m\mu\rangle \,, \tag{11}$$

and θ the angle of the outgoing η meson with respect to the incoming photon momentum. Here we have assumed covariant state normalization, i.e.,

$$\langle p'|p\rangle = (2\pi)^3 \frac{E_p}{M} \delta(\vec{p}' - \vec{p}) \tag{12}$$

for fermions and

$$\langle p'|p\rangle = (2\pi)^3 2\omega_p \delta(\vec{p}' - \vec{p}) \tag{13}$$

for bosons.

Besides the dominant S_{11} resonance in the s-channel, we consider for the t-matrix the S_{11} in the u-channel, the nucleon pole terms in the s- and u-channels, as well as ρ and ω exchange in the t-channel as background contributions. The corresponding diagrams are shown in Fig. 1. All vertices are calculated from the following effective Lagrangians [16]

$$\mathcal{L}_{\eta NN}^{PS} = -ig_\eta \bar{\Psi} \gamma_5 \Psi \phi_\eta \,, \tag{14}$$

$$\mathcal{L}_{\gamma NN} = -e\bar{\Psi} \gamma_\mu \frac{1 + \tau_0}{2} \Psi A^\mu - \frac{e}{4M} \bar{\Psi}(\kappa^s + \kappa^\nu \tau_0) \sigma_{\mu\nu} \Psi F^{\mu\nu} \,, \tag{15}$$

$$\mathcal{L}_{VNN} = -g_v \bar{\Psi}\gamma_\mu \Psi V^\mu - \frac{g_t}{4M}\bar{\Psi}\sigma_{\mu\nu}\Psi V^{\mu\nu}\,, \tag{16}$$

$$\mathcal{L}_{V\eta\gamma} = \frac{e\lambda}{4m_\eta}\varepsilon_{\mu\nu\lambda\sigma}F^{\mu\nu}V^{\lambda\sigma}\phi_\eta\,, \tag{17}$$

$$\mathcal{L}_{\eta N S_{11}} = -ig_{\eta N S_{11}}\bar{\Psi}\Psi_{S_{11}}\phi_\eta + h.c\,, \tag{18}$$

$$\mathcal{L}_{\gamma N S_{11}} = -\frac{e}{2(M_{S_{11}} + M)}\bar{\Psi}_{S_{11}}(\kappa^s_{res} + \kappa^v_{S_{11}}\tau_0)\gamma_5\sigma_{\mu\nu}\Psi F^{\mu\nu} + h.c.\,. \tag{19}$$

Here, Ψ and $\Psi_{S_{11}}$ describe the fermion fields of the nucleon and the S_{11} resonance, respectively, V^μ the vector meson field, ϕ_η the pseudoscalar eta meson field, and A^μ the photon field with its field tensor $F^{\mu\nu}$. The vector meson field tensor is analogously defined by $V^{\mu\nu} = \partial^\mu V^\nu - \partial^\nu V^\mu$. The S_{11} mass is denoted by $M_{S_{11}}$ and the isoscalar (isovector) anomalous magnetic moment of the nucleon by κ^s (κ^v).

For the the ηNN-vertex we have chosen the pseudoscalar coupling [5,21]. Values of the coupling constant range usually between 0 and 7 [16,21]. Fitting the model to the data, we find as best choice $\frac{g_\eta^2}{4\pi} = 0.4$ in good agreement with results from [5] and with a recent calculation by Kirchbach and Tiator [22] evaluating an effective ηNN-vertex associated with the $a_0(980)\pi N$ triangle diagram. The coupling constant λ of the $V\eta\gamma$-vertex can be determined from the known electromagnetic decay $V \to \gamma\eta$, with $V = \rho$ or ω. Here we use $\Gamma_{\rho\to\gamma\eta} = 57.46$ MeV and $\Gamma_{\omega\to\gamma\eta} = 3.96$ MeV [20]. At the hadronic VNN-vertex, a phenomenological form factor $F(\vec{q}_V)$ of dipole type is introduced

$$F(\vec{q}_V) = \frac{(\Lambda_V^2 - m_V^2)^2}{(\Lambda_V^2 + \vec{q}_V{}^2)^2}, \tag{20}$$

with $\vec{q}_V$ being the momentum of the vector meson and Λ_V the cut-off mass. A more detailed description, also for the coupling constants of the hadronic vertex g_v and g_t, may be found in [17] and references therein. Table I summarizes all parameters used for the vector mesons.

The photoexcitation of the S_{11} resonance can be described by the helicity amplitudes $A_{1/2}^{p,n}$ (with upper index p referring to the proton, n to the neutron) which may be split into isoscalar and isovector amplitudes by

$$A_{1/2}^{p,n} = A_{1/2}^s \pm A_{1/2}^v\,. \tag{21}$$

6

They determine the resonance parameters $\kappa_{S_{11}}^{s/v}$ in (19) and are related to the helicity amplitudes $A_{1/2}^{s/v}$ by

$$e\kappa_{S_{11}}^{s/v} = \sqrt{\frac{2M(M_{S_{11}} + M)}{M_{S_{11}} - M}} A_{1/2}^{s/v}. \tag{22}$$

Furthermore, the $\eta N S_{11}$-coupling constant is given by

$$\frac{g_{\eta N S_{11}}^2}{4\pi} = \frac{2M_{S_{11}}^2}{q_\eta^*((M_{S_{11}} + M)^2 - m_\eta^2)}\Gamma_{S_{11}}^0, \tag{23}$$

where q_η^* is the η momentum at resonance in the ηN c.m. frame, given by (9) for $s = M_{S_{11}}^2$, and $\Gamma_{S_{11}}^0$ denotes the S_{11} decay width. The resonance mass $M_{S_{11}}$, the helicity amplitudes $A_{1/2}^{p,n}$, the hadronic coupling $g_{\eta N S_{11}}$ and the decay width $\Gamma_{S_{11}}^0$ are only known within large uncertainties [5,19]. For the resonance, we use the free propagator in the form

$$\left[W_{\gamma N} - M_{S_{11}} + \frac{i}{2}\Gamma_{S_{11}}(W_{\gamma N})\right]^{-1}. \tag{24}$$

The S_{11} resonance mainly decays into $N\eta$ (50 %), $N\pi$ (40 %), and $N\pi\pi$ (10 %) [19]. Consequently, one has for the total decay width at resonance position

$$\Gamma_{S_{11}}(M_{S_{11}}) = \Gamma_{S_{11} \to \eta N} + \Gamma_{S_{11} \to \pi N} + \Gamma_{S_{11} \to \pi\pi N} \tag{25}$$

$$= 0.5\Gamma_{S_{11}}^0 + 0.4\Gamma_{S_{11}}^0 + 0.1\Gamma_{S_{11}}^0. \tag{26}$$

In (24) we already have introduced an energy dependend decay width $\Gamma_{S_{11}}(W_{\gamma N})$ depending on the invariant mass $W_{\gamma N}$ of the system since it gives a much better description of experimental data than using a constant width. For the two leading decay channels, we have calculated the corresponding partial decay widths from the Lagrangians in first order perturbation theory, whereas the three body decay $S_{11} \to \pi + \pi + N$ is treated on a purely phenomenological level keeping it constant above its threshold. Then we have for the total width as function of the invariant mass

$$\begin{aligned}
\Gamma_{S_{11}}(W_{\gamma N}) = {} & \frac{g_{\eta N S_{11}}^2 M}{2\pi W_{\gamma N}} q_\eta(W_{\gamma N})\Theta(W_{\gamma N} - W_{\eta N}^{th}) \\
& + \frac{g_{\pi N S_{11}}^2 M}{2\pi W_{\gamma N}} q_\pi(W_{\gamma N})\Theta(W_{\gamma N} - W_{\pi N}^{th}) \\
& + 0.1\Gamma_o\Theta(W_{\gamma N} - W_{\pi\pi N}^{th}).
\end{aligned} \tag{27}$$

Here, $q_\eta(W_{\gamma N})$ is given by (9) and $q_\pi(W_{\gamma N})$ by the analogous equation replacing m_η by m_π. The threshold masses for the decay channels are correspondingly denoted by $W_{\eta N}^{th}$, $W_{\pi N}^{th}$ and $W_{\pi\pi N}^{th}$. The coupling constants $g_{\eta N S_{11}}$ and $g_{\pi N S_{11}}$ are fixed by evaluating the partial decay widths at resonance position.

In Table II we list the set of resonance parameters for which we obtain the best fit [23] to the total cross section data as can be seen in Fig. 2. Only above 850 MeV, the theoretical cross section overestimates the data. The differential cross sections calculated with these parameters are shown in Fig. 3. While at lower energies the angular dependence is quite satisfactory, one finds larger deviations at higher energies. One reason for this might be the omission of the D_{13} resonance [17,21]. However, for the present study this is of no relevance.

III. THE COHERENT PROCESS ON THE DEUTERON

Now we turn to the coherent η production on the deuteron

$$\gamma(k_\mu) + d(d_\mu) \to \eta(q_\mu) + d(d'_\mu) \,. \tag{28}$$

The variables in parentheses refer to the corresponding four momenta of the particles. We will consider this reaction in the photon-deuteron (γd) c.m. frame. There we choose the z-axis along the photon momentum $(\vec{e}_z = \hat{k} = \vec{k}/k)$, the y-axis parallel to $\vec{k} \times \vec{q}$ and the x-axis such as to form a right handed system. Thus the outgoing η meson is described by the spherical angles $\phi = 0$ and θ with $\cos\theta = \hat{q} \cdot \hat{k}$.

For the unpolarized differential cross section we obtain in the γd c.m. frame [23]

$$\frac{d\sigma}{d\Omega_\eta^{c.m.}} = \frac{1}{6} \frac{1}{16\pi^2} \frac{q}{k} \frac{E_k^d E_q^d}{W_{\gamma d}^2} \sum_{m_d m'_d \mu} |\tau_{m_d m'_d \mu}(W_{\gamma d}, \theta)|^2 \,, \tag{29}$$

with $E_p^d = \sqrt{M_d^2 + \vec{p}^2}$. Here we have introduced as t-matrix

$$\tau_{m_d m'_d \mu}(W_{\gamma d}, \theta) = \langle m'_d | t_{\gamma\eta}^d(W_{\gamma d}) | m_d \mu \rangle \,, \tag{30}$$

denoting the initial and final deuteron spin projections by m_d and m'_d, respectively, and the photon polarization by μ. Furthermore, $W_{\gamma d}$ denotes the invariant mass of the γd system

and k and q again the photon and η momentum, respectively, in the γd c.m. system. These quantities are given as function of the lab photon energy by expressions analogous to (7) through (9) replacing the nucleon mass M by the deuteron mass M_d. Here the η production threshold is at $E_\gamma^{Lab} = 629$ MeV, which is equivalent to an invariant mass $W_{\gamma d}^{thr} = 2424$ MeV.

As noted in the introduction, we restrict our calculation to the impulse approximation which means that the reaction will take place only on one of the two nucleons leaving the other as a pure spectator (see the diagram in Fig. 4). Consequently, the production operator $t_{\gamma\eta}^d$ for the reaction on the deuteron is obtained from the elementary operator $t_{\gamma\eta}$ by

$$t_{\gamma\eta}^d = t_{\gamma\eta}^{(1)} \times \mathbb{1}^{(2)} + \mathbb{1}^{(1)} \times t_{\gamma\eta}^{(2)} \,, \tag{31}$$

where the upper index in brackets refers to the nucleon on which the operator acts. Off-shell effects will be neglected. Then the t-matrix has the following form

$$\tau_{m_d m_d' \mu} = 2 \sum_{m_s', m_s} \int d^3 p \, \psi_{m_s' m_d'}^* \left(\vec{p} - \frac{\vec{q}}{2} \right) \langle \vec{p} - \vec{q}; 1 m_s', 00 | t_{\gamma\eta}^{(1)} | \vec{p} - \vec{k}; 1 m_s, 00 \rangle \psi_{m_s m_d} \left(\vec{p} - \frac{\vec{k}}{2} \right), \tag{32}$$

where $|1 m_s, 00\rangle$ denotes the two-nucleon spin and isospin wave function. Here, the intrinsic part of the deuteron wave function projected onto $|1 m_s\rangle$ is denoted by

$$\psi_{m_s m_d}(\vec{p}) = \sum_{l=0,2} \sum_{m_l} (l m_l 1 m_s | 1 m_d) i^l u_l(p) Y_{l,m_l}(\hat{p}) \,. \tag{33}$$

For the radial wave functions u_0 and u_2, we have taken the ones of the Bonn r-space potential [24].

The operator $t_{\gamma\eta}^{(1)}$ is a function of the photon, nucleon and eta momenta $\vec{k}$, $\vec{p}$, and $\vec{q}$, respectively, the photon polarization μ, and the invariant mass $W_{\gamma N}$ of the photon-nucleon subsystem. As already mentioned in the introduction, implementing this operator into a bound system poses two problems. First of all, one has to know the invariant mass $W_{\gamma N}$ for the struck or active nucleon, and secondly, one needs the elementary t-matrix not in the γN c.m. system but in an arbitrary frame of reference. We will discuss these two points now in some detail.

A. Choices for the invariant mass $W_{\gamma N}$ for the γN subsystem

For a bound system of two nucleons, the general expression for $W_{\gamma N}$ is, assuming the reaction to take place at nucleon "1",

$$
\begin{aligned}
W_{\gamma N} &= \sqrt{(p_{10} + k_0)^2 - (\vec{p}_1 + \vec{k})^2} \\
&= \sqrt{(p'_{10} + \omega_q)^2 - (\vec{p}_1{}' + \vec{q})^2},
\end{aligned}
\tag{34}
$$

where $p_{1\mu}^{(\prime)} = (p_{10}^{(\prime)}, \vec{p}_1^{(\prime)})$ denotes its initial (final) four momentum. In general, one has $p_{10}^{(\prime)} \neq \sqrt{M^2 + \vec{p}^{\,(\prime)2}}$. In fact, the energy of an individual bound nucleon of a nonrelativistic many-particle system is not well defined. Only the total sum of the energies of all nucleons is a well defined quantity, e.g., for the deuteron $E^{d^{(\prime)}} = p_{10}^{(\prime)} + p_{20}^{(\prime)}$.

One of many possible choices is to distribute the total energy of the deuteron equally on each of the two nucleons (Blankenbecler-Sugar choice) in the deuteron rest system, i.e., each nucleon has the energy $M_d/2$, independent of the momentum. Making such an assignment for the initial two nucleons, the boost to the γd c.m. system gives then with $\vec{p}_1 = \vec{p} - \vec{k}$

$$
W_{\gamma N}^{BS} = \frac{1}{E_k^d} \sqrt{\left(\frac{1}{2}(E_k^d + k_0)^2 - \vec{k} \cdot \vec{p}\right)^2 - \vec{p}^{\,2}(E_k^d)^2}\,,
\tag{35}
$$

while for the final two nucleons one finds

$$
W_{\gamma N}^{BS'} = \frac{1}{E_q^d} \sqrt{\left(\frac{1}{2}(E_q^d + \omega_q)^2 - \vec{q} \cdot \vec{p}\right)^2 - \vec{p}^{\,2}(E_q^d)^2}\,.
\tag{36}
$$

Another possibility is to take the active nucleon on-shell either before or after the interaction. In the first case, one finds with $p_{10} = E_{p-k} = \sqrt{M^2 + (\vec{p} - \vec{k})^2}$

$$
W_{\gamma N}^{N} = \sqrt{(k_0 + E_{p-k})^2 - \vec{p}^{\,2}}\,,
\tag{37}
$$

whereas in the second case with the final nucleon on-shell, i.e. $p'_{10} = E_{p-q} = \sqrt{M^2 + (\vec{p} - \vec{q})^2}$, one has

$$
W_{\gamma N}^{N'} = \sqrt{(\omega_q + E_{p-q})^2 - \vec{p}^{\,2}}\,.
\tag{38}
$$

The former choice has been made in [21]. In all these three cases, the invariant mass depends on the kinematics, i.e., for fixed nucleon momentum on the angle between $\vec{p}$ and the outgoing η momentum $\vec{q}$.

The last choice, we want to discuss is to put the spectator nucleon on-shell, i.e., $p_{20} = E_p$. This choice has been taken in [9]. It is also used in coherent π^0 photoproduction on the deuteron [25], and it may be justified by the fact that the deuteron is only loosely bound, and hence the spectator acts nearly like a free nucleon. We obtain in this case

$$W_{\gamma N}^{S} = \sqrt{(W_{\gamma d} - E_p)^2 - \vec{p}^2}\,, \tag{39}$$

which is independent from the direction of $\vec{p}$.

Figure 5 shows the invariant mass $W_{\gamma N}$ for these different choices as function of the spectator momentum at fixed photon lab energy $E_\gamma^{Lab} = 800$ MeV. For the first four choices ($W_{\gamma N}^{BS}$, $W_{\gamma N}^{BS'}$, $W_{\gamma N}^{N}$ and $W_{\gamma N}^{N'}$) we have represented the boundaries of the range spanned by the angle dependence by two curves corresponding to $\vec{p}$ and $\vec{k}$ or $\vec{q}$ parallel (upper curve) and antiparallel (lower curve). One readily notes that $W_{\gamma N}^{N}$ spans the largest range, while the smaller ranges of $W_{\gamma N}^{BS}$, $W_{\gamma N}^{BS'}$ and $W_{\gamma N}^{N'}$ are compatible with each other. However, the average invariant masses nearly coincide for $W_{\gamma N}^{N}$ and $W_{\gamma N}^{N'}$, and they show a slight increase with increasing spectator momentum, whereas it decreases for both $W_{\gamma N}^{BS}$ and $W_{\gamma N}^{BS'}$ which, moreover, show a very similar behaviour. Finally, $W_{\gamma N}^{S}$ gives the lowest invariant mass with the strongest decrease with increasing p. One has to keep in mind that the main contribution to the total cross section originates from momenta p below 400 MeV. But even in this region one notes a sizeable difference between the various choices for the invariant mass of the active γN subsystem.

B. Contribution of ω meson exchange in an arbitrary reference frame

Now we will illustrate for the case of ω meson exchange the two methods for deriving the elementary production operator for a general frame of reference as mentioned above.

11

To this end, we evaluate first the corresponding Feynman diagrams for an arbitrary frame (see the Appendix). The resulting t-matrix is expressed in terms of two amplitudes $\tilde{M}_v$ and $\tilde{M}_t$ which are also defined in the Appendix. These in turn can be represented as linear combinations of the following operators

$$\Omega^0_{\vec{a}, \vec{b}} := i\vec{\varepsilon} \cdot (\vec{a} \times \vec{b}), \qquad \Omega^1 := \vec{\sigma} \cdot \vec{\varepsilon}, \qquad \Omega^2_{\vec{a}, \vec{b}} := \vec{\sigma} \cdot \vec{a}\, \vec{\varepsilon} \cdot \vec{b}. \tag{40}$$

We then specialize to the γd c.m. system by the replacements $\vec{p} \to \vec{p} - \vec{k}$ and $\vec{p}' \to \vec{p} - \vec{q}$, so that the γN subsystem moves with the total momentum $\vec{p}$. The corresponding coefficients for the amplitudes $\tilde{M}_v$ and $\tilde{M}_t$ are listed in Tab. III where s, t and u stand for the Mandelstam variables of the γN subsystem. We further have introduced $p_0 = \sqrt{\vec{p}^2 + s}$, the total energy of the subsystem, $E = \sqrt{(\vec{p} - \vec{k})^2 + M^2}$ and $E' = \sqrt{(\vec{p} - \vec{q})^2 + M^2}$, the on-shell energies of the initial and final active nucleon, respectively, and $e_\pm = e' \pm e$ with $e^{(\prime)} = E^{(\prime)} + M$.

Then, in order to proceed according to the second method, we specialize to the γN c.m. frame. Here one usually expresses the t-matrix in terms of the CGLN amplitudes. But we prefer to give them in terms of the operators defined in (40), i.e.

$$\vec{\sigma} \cdot \vec{k}\, \vec{\varepsilon} \cdot \vec{q} = \Omega^2_{\vec{k}, \vec{q}}, \tag{41}$$

$$\vec{\sigma} \cdot \vec{q}\, \vec{\varepsilon} \cdot \vec{q} = \Omega^2_{\vec{q}, \vec{q}}, \tag{42}$$

$$i\vec{\sigma} \cdot \vec{q}\, \vec{\sigma} \cdot (\vec{k} \times \vec{\varepsilon}) = -\Omega^0_{\vec{k}, \vec{q}} - \vec{k} \cdot \vec{q}\,\Omega^1 + \Omega^2_{\vec{k}, \vec{q}}. \tag{43}$$

We list the resulting coefficients in Tab. IV. These operators are then transformed to the γd c.m. frame by a proper Lorentz boost of all participating momenta, i.e., we boost $\vec{k}_{c.m.}$ and $\vec{q}_{c.m.}$ defined with respect to the γN c.m. frame to $\vec{k}$ and $\vec{q}$ with respect to the γd c.m. frame. In the latter frame the γN system moves with momentum $\vec{p}$ according to our choice of variables (see Fig. 4). Then the Lorentz transformation reads

$$\vec{k}_{c.m.} = \vec{k} + A_k \vec{p}, \tag{44}$$

$$\vec{q}_{c.m.} = \vec{q} + A_q \vec{p}, \tag{45}$$

with the boost parameter

12

$$A_k = \frac{1}{W_{\gamma N}} \left(\frac{\vec{k} \cdot \vec{p}}{E_{\gamma N} + W_{\gamma N}} - k_0 \right), \tag{46}$$

where $E_{\gamma N} = \sqrt{W_{\gamma N}^2 + \vec{p}^2}$ denotes the energy of the γN subsystem, and A_q is given by a corresponding expression replacing k_μ by q_μ in (46). Expressing k_0 and ω_q in terms of the invariant mass, the energy and the total momentum of the subsystem

$$k_0 = \frac{1}{2E_{\gamma N}} \left(W_{\gamma N}^2 - M^2 + 2\vec{k} \cdot \vec{p} \right), \tag{47}$$

$$\omega_q = \frac{1}{2E_{\gamma N}} \left(W_{\gamma N}^2 - M^2 + m_\eta^2 + 2\vec{q} \cdot \vec{p} \right), \tag{48}$$

we find for the boost parameters

$$A_k = -\frac{1}{2W_{\gamma N} E_{\gamma N}} \left(W_{\gamma N}^2 - M^2 + \frac{2W_{\gamma N}}{E_{\gamma N} + W_{\gamma N}} \vec{k} \cdot \vec{p} \right), \tag{49}$$

$$A_q = -\frac{1}{2W_{\gamma N} E_{\gamma N}} \left(W_{\gamma N}^2 + m_\eta^2 - M^2 + \frac{2W_{\gamma N}}{E_{\gamma N} + W_{\gamma N}} \vec{q} \cdot \vec{p} \right), \tag{50}$$

For the resulting transformation of the operators we find

$$\Omega^0_{\vec{k}, \vec{q}} \rightarrow \Omega^0_{\vec{k}, \vec{q}} + A_k \, \Omega^0_{\vec{p}, \vec{q}} + A_q \, \Omega^0_{\vec{k}, \vec{p}}, \tag{51}$$

$$\Omega^1 \rightarrow \Omega^1, \tag{52}$$

$$\Omega^2_{\vec{k}, \vec{q}} \rightarrow \Omega^2_{\vec{k}, \vec{q}} + A_k \, \Omega^2_{\vec{p}, \vec{q}} + A_q \, \Omega^2_{\vec{k}, \vec{p}} + A_k A_q \, \Omega^2_{\vec{p}, \vec{p}}, \tag{53}$$

$$\Omega^2_{\vec{q}, \vec{q}} \rightarrow \Omega^2_{\vec{q}, \vec{q}} + A_q \, \Omega^2_{\vec{p}, \vec{q}} + A_q \, \Omega^2_{\vec{q}, \vec{p}} + A_q^2 \, \Omega^2_{\vec{p}, \vec{p}}, \tag{54}$$

leading to the same operator structures as for the general case. However, they differ in their corresponding coefficient functions as can already be seen by comparing the first four operators in Tab. III with the corresponding ones in Tab. IV which are not affected by the transformation. They differ just by terms which vanish in the γN c.m. frame. Thus it is not surprising that these terms cannot be generated by a boost. This means that information has been lost when going first to the γN c.m. frame with subsequent boost. Furthermore, for the remaining operators, which vanish in the γN c.m. frame, one finds little resemblance between the two methods. For example, the coefficient of $\Omega^2_{\vec{p}, \vec{p}}$ in $\tilde{M}_v$ vanishes in Tab. III whereas the one resulting from the transformation of $\Omega^2_{\vec{k}, \vec{q}}$ and $\Omega^2_{\vec{q}, \vec{q}}$ does not vanish. In Sect. IV we will discuss the effect of these differences on the cross sections.

13

IV. RESULTS AND DISCUSSION

Having fixed the parameters of the η production model for the elementary process we can now proceed to study the coherent reaction on the deuteron. The t-matrix elements of (32) have been evaluated numerically using Gauss integration in momentum space. As deuteron wave functions, we have taken the ones of the Bonn r-space potential [24]. With respect to the elementary amplitudes, only the value for the helicity amplitude of the neutron $A^n_{1/2}$ remained undetermined. We have listed several values for $A^n_{1/2}$ in Table V to be discussed in the following together with the resulting ratios of the neutron to proton amplitude $A^n_{1/2}/A^p_{1/2}$ and the correlated values for $e\kappa^s_{S_{11}}$ and the ratio of the isoscalar to the proton amplitude $A^s_{1/2}/A^p_{1/2} = 1 + \frac{A^n_{1/2}}{A^p_{1/2}}$. In addition, the last line of Table V summarizes the range of values for these quantities which can be found in the literature ([10,13,19] and references therein) and which are obtained either from photo reactions or from quark model predictions.

First, we will consider the experimental results of Krusche et al. [13] in order to discuss the limits on the neutron amplitude $A^n_{1/2}$ as imposed by present experimental data. Krusche et al. have measured the total and differential cross sections for quasifree η photo production on the deuteron for energies from threshold up to 800 MeV, and they found for the ratio of neutron to proton total cross sections a value $\frac{\sigma_n}{\sigma_p} \simeq \frac{2}{3}$. Furthermore, they have estimated from their data for the neutron resonance amplitude $A^n_{1/2} = -(100 \pm 30) \cdot 10^{-3} \mathrm{GeV}^{-\frac{1}{2}}$ and for the cross section of the coherent process a value $(10^{-3} \pm 10^{-2})\,\mu\mathrm{b/sr}$. This clearly indicates that the excitation of the S_{11} resonance is dominated by the isovector amplitude. Consequently, the neutron and proton helicity amplitudes should have opposite sign, i.e.,

$$A^n_{1/2} = \pm\sqrt{\frac{\sigma_n}{\sigma_p}}A^p_{1/2}\,. \tag{55}$$

With our choice of $A^p_{1/2} = 130 \cdot 10^{-3}\mathrm{GeV}^{-\frac{1}{2}}$ (Table II) we get $A^n_{1/2} = -106 \cdot 10^{-3}\mathrm{GeV}^{-\frac{1}{2}}$. It corresponds to the parameter set (A) in Table V. The differential cross sections corresponding to this value of $A^n_{1/2}$ are shown in Fig. 6 for four different photon lab energies E^{Lab}_γ. The results are well within the limit given by [13] for the coherent production on the deuteron.

14

Fig. 7 shows the differential cross sections at a photon lab energy $E_\gamma^{Lab} = 700$ MeV for the choices (A) through (C) for $A_{1/2}^s/A_{1/2}^p$ listed in Table V and, for comparison, the result of Tiator et al. [21]. We have also indicated separately the contributions of the resonance and the nucleon Born terms. One readily sees the strong sensitivity on $\kappa_{S_{11}}^s$. An increase of $\kappa_{S_{11}}^s$ by a factor of two ((A) $\rightarrow$ (C)) leads to an increase of the cross section by almost a factor four. One also notes a destructive interference between resonance and nucleon pole term contributions whereas the vector meson exchange terms lead to a slight increase. Case (A) corresponds to the already discussed estimate of Krusche et al. while (B) is motivated by quark model predictions. Taking these as upper limit, then remains for the ratio $A_{1/2}^s/A_{1/2}^p$ only the value 0.14 (set (B) in Table V). The next case (C) serves for comparison with [21]. If we take the same ratio for $A_{1/2}^s/A_{1/2}^p$ as in [21], namely 0.15 which is very close to set (B) in Table V, we get only 75 % of their result. However, doubling the ratio of set (A), yielding set (C) of Table V, we find a cross section that is qualitatively equal to the one of [21]. However, our angular distribution drops somewhat faster with increasing angle than the one of [21].

The main differences between our calculation and the one of Tiator et al. [21] are that (i) they include in addition the resonances P_{11} and D_{13}, but all resonances only in the s-channel, (ii) their elementary production model is a mixture of the isobar model and a coupled channel calculation, (iii) they start from the CGLN amplitudes in the γN c.m. frame and then boost all momenta as described above, (iv) they do not integrate over the spectator momentum but make use of the so-called factorization approximation which leads to uncertainties of about 5 to 10 % [26], (v) they have used an ηN-coupling constant for the nucleon Born terms of $g_\eta^2/4\pi = 0.1$ in contrast to our value of 0.4, and (vi) they have chosen $W_{\gamma N}^{N'}$ as invariant mass of the γN subsystem.

The earlier experiment of Anderson and Prepost [7] seemed to indicate that the isoscalar amplitude of the resonance is the dominant part instead of the isovector one in contradiction to quark model predictions which give $A_{1/2}^s/A_{1/2}^p \simeq (-0.02 \pm 0.16)$ (see [10] and references therein). In fact, the calculations of [8] in the impulse approximation require for this ratio

a much larger value of 0.84 in order to reproduce the data of [7]. Even if one considers pion and eta rescattering terms one still needs a value of 0.6 [10]. In our approach, we could reproduce the data of [7] with a value of 0.88 corresponding to $A_{1/2}^n = 114 \cdot 10^{-3}\mathrm{GeV}^{-\frac{1}{2}}$ and $e\kappa_{S_{11}}^s = 340 \cdot 10^{-3}\mathrm{GeV}^{-\frac{1}{2}}$ as is shown in Fig. 8. On the other hand, the data of [7] are obviously at variance with the measurements of [13] mentioned above which clearly prefer the isovector part to be the dominant one. This is also supported by comparing our results with the upper limit near threshold obtained by Beulertz [12] which will be discussed in more detail next. The cross section exceeds this upper limit by more than a factor four. This fact and more recent experiments with a better background reduction imply that very likely the experiment [7] has included other events and therefore has resulted in an overestimation of the η production cross section.

Now we will study the question for which values of $A_{1/2}^n$ in Table V the resulting total cross section is compatible with the upper limits obtained by Beulertz [12]. Instead of detecting the η meson by its two-photon decay as, for example, is done by [13], the recoiling deuteron has been used as signal and the upper limits $\sigma_{tot} < 0.040\,\mu\mathrm{b}$ for $E_\gamma^{Lab} = 632.2$ MeV and $< 0.064\,\mu\mathrm{b}$ for $E_\gamma^{Lab} = 637$ MeV have been obtained. In Fig. 9 we show theoretical total cross sections for the six different values of $A_{1/2}^n$ for the parameter sets (A) through (F) of Table V. Although these resonance couplings vary over a wide range, the variation in the total cross sections is much less pronounced in the near threshold region than at higher energies. Even a sign change in $e\kappa_{S_{11}}^s$ does not show a big influence as one can see by comparing the results of set (C) with (E) or (D) with (F) except above the resonance region where the interference with the background becomes more important. The experimental upper limit is reached for the set (G) as is shown in Fig. 10.

All parameter sets of Table V give total cross sections compatibel with the experimental estimates for the coherent deuteron cross section of [12] and [13]. However, if one takes the quark model seriously, the parameter sets (D) through (G) can be excluded while (C) is on the borderline. Thus we conclude that the most probable parameter sets are (A) through

(C) which give a neutron amplitude $A_{1/2}^n$ between $-82 \cdot 10^{-3}$ and $-106 \cdot 10^{-3} \text{GeV}^{-\frac{1}{2}}$. The set (A) reproduces the experimental ratio for $\sigma_n/\sigma_p = 2/3$ [13], whereas we find the best agreement with the theoretical results of [21] for the set (C). In this case, the ratio of neutron to proton cross section is only $2/5$.

Now we want to discuss the influence of different choices for the invariant mass of the γN subsystem. Figure 11 presents the total cross sections for the S_{11} resonance alone obtained with four of the different choices for the invariant mass $W_{\gamma N}$ as discussed in Sect. III. We did not consider $W_{\gamma N}^{BS'}$ because it is very similar to $W_{\gamma N}^{BS}$. Since for this question the exact value of $A_{1/2}^n$ is not relevant, we have used here $A_{1/2}^n = -82 \cdot 10^{-3} \text{GeV}^{-\frac{1}{2}}$. One readily notes considerable differences for the various prescriptions. The largest total cross section is obtained with the spectator on shell $W_{\gamma N}^S$ having its maximum at 750 MeV. If one puts the active nucleon on shell, i.e., takes $W_{\gamma N}^N$ or $W_{\gamma N}^{N'}$ instead, the maximum is decreased by about 18% and slightly shifted towards higher energies.

This decrease and shift can be understood as a result of the assignment of a higher invariant mass to the γN subsystem and the additional smearing due to the dependence on the angle between the spectator momentum and the photon, respective eta momentum (see Fig. 5) which leads to a larger effective width. The result is a slight upshift of the resonance position and a broadening, thus lowering of the maximum. One notes also little difference between putting the active nucleon before or after the interaction on shell. From the foregoing discussion it is apparent that the curve for the Blankenbecler-Sugar assignment $W_{\gamma N}^{BS}$ is about halfway between the spectator on shell and the active nucleon on shell because according to Fig. 5 $W_{\gamma N}^{BS}$ lies in between the spectator and active nucleon assignments.

The differential cross sections for three photon energies in Fig. 12 show a similar behaviour with respect to the invariant mass assignment. In particular at lower energies (see as example the cross section at $E_\gamma = 700$ MeV in Fig. 12) the differences are quite sizeable in forward direction.

In view of these results, we have to conclude that the choice for the invariant mass of

17

the γN subsystem has a significant influence on the cross section. In order to obtain a cross section of the same magnitude for two different choices of $W_{\gamma N}$, one has to change the elementary helicity amplitude, too. Consequently, the other correlated parameters (see Table V) will change together with the assignment for the invariant mass. This has also some bearing on the question of compatibility with quark model predictions.

As last point we want to discuss the different methods of deriving the elementary production operator in an arbitrary frame which is necessary for implementing it into the bound system, i.e., we will compare the more general case using an arbitrary frame (GC), the Lorentz boost of the momenta from the γN c.m. frame (LB), and the simplest approach of taking the elementary operator without any transformation of the variables (CM). The last method, for example, is considered in [27] for the coherent π^0 photoproduction on the deuteron where only the momentum of the Δ resonance is transformed while for the background terms this has not been done, assuming the effect to be negligible. While for the pion this might be justified because of its low mass, one certainly would not expect it to be a valid approximation for the eta meson.

We present results for two choices of the neutron helicity amplitude, namely $A_{1/2}^n = -106 \cdot 10^{-3} \text{GeV}^{-\frac{1}{2}}$ (A) and $A_{1/2}^n = -82 \cdot 10^{-3} \text{GeV}^{-\frac{1}{2}}$ (C) (Table V). The differential cross sections as a function of the photon laboratory energy and for constant c.m. angles are shown for both amplitudes in Figs. 13. It can be seen that the differences between (GC), (LB), and (CM) depend not only on the angles and energies but also on the strength of the helicity amplitude chosen.

Comparing first (GC) and (LB), we see that at forward angles the deviations are small. However, for backward angles they become more significant reaching a maximum at 180°. The maximum is considerably lower for (LB) while at higher energies the differential cross setion for (LB) lies above the one for (GC). On the other hand, the main contributions to the cross sections stem from small angles where also the differences are smaller so that the total cross sections differ much less. Furthermore, using a larger helicity amplitude $A_{1/2}^n$ decreases the differences between the calculations (GC) and (LB) even more. That is the

case for an $A_{1/2}^n$ with which we get a cross section comparable to the one of [21].

Finally, comparing the calculation (CM), to which only the first four operator structures of Table III contribute, with (GC) one clearly sees very large deviations from (GC) which obviously are not tolerable.

V. SUMMARY AND CONCLUSIONS

Coherent eta photoproduction on the deuteron has been studied in the impulse approximation neglecting rescattering and two-body effects. For the elementary reaction, we have assumed that the process is dominated by the excitation of the $S_{11}(1535)$ resonance for photon energies not too far above threshold. Thus we have included the S_{11} in the s- and u-channels. In addition, we have considered as background the t-channel vector meson exchange with ρ and ω as well as the nucleon pole terms in s- and u-channel for which pseudoscalar coupling has been assumed. The vertices are taken from an effective Lagrangian theory. The elementary process is treated nonrelativistically. All parameters are fixed by fitting the experimental data for the reaction on the proton.

The electromagnetic coupling constant $A_{1/2}^n$ for the S_{11} excitation on the neutron cannnot be determined this way, and one needs data for the reaction on the deuteron. In view of the fact that up to now no precise data on the deuteron are available, we could only use the existing estimates to find limits for this amplitude. The experiment for quasifree production [13] gave a value for the ratio of neutron to proton cross section with which we have obtained a deuteron cross section that is within the experimentally obtained limits of [12] and [13]. Correlated with this is a ratio of the isoscalar to isovector amplitude that is consistent with quark model predictions. However, the upper limits of [12] and [13] for the coherent deuteron cross section are not sufficient for a precise determination of $A_{1/2}^n$. An uncertainty of the factor ten is to be considered which could result in deviations from quark model predictions up to 50%. Furthermore, we have studied the theoretical problems of implementing the elementary reaction amplitude into a bound system connected to the choice of the invariant

19

mass for the resonance excitation and to the transformation of the reaction amplitude from the γN c.m. frame to the c.m. frame of the γ-bound system, and we have found that the theoretical results show significant differences when using different prescriptions.

For the future we need on the experimental side precise data for both the coherent and the incoherent production on the deuteron in order to be able to fix in a reliable manner the S_{11} excitation on the neutron. On the theoretical side, we have to improve the treatment by including rescattering and two-body effects in order to obtain a more realistic description of this important process.

APPENDIX: T-MATRIX CONTRIBUTION FROM ω MESON EXCHANGE

With the aid of the Lagrangians (16)-(17) we get for the t-matrix contribution from vector meson exchange

$$i\tau_{fi}^V = \frac{e\lambda}{m_\eta} \frac{\varepsilon_{\mu\nu\lambda\sigma} k^\nu \varepsilon^\mu q^\lambda}{t - m_V^2} \bar{u}_f(p') \left[g_v \gamma^\sigma - \frac{g_t}{2M} i\sigma^{\sigma\alpha}(q-k)_\alpha \right] u_i(p) \,. \tag{A.1}$$

For the ρ meson one has to multiply with an additional factor τ_0. In the CGLN-representation [28], on has for photo production only four independent amplitudes

$$i\tau_{fi} = \bar{u}_f(p') \sum_{j=1}^{4} A_j(s,t,u) M_j u_i(p) \,. \tag{A.2}$$

containing the Dirac operators

$$M_1 = -\frac{1}{2}\gamma_5 \gamma_\mu \gamma_\nu (\epsilon^\mu k^\nu - \epsilon^\nu k^\mu) \,, \tag{A.3}$$

$$M_2 = \gamma_5 (p+p')_\mu \left(q_\nu - \frac{1}{2}k_\nu \right) (\epsilon^\mu k^\nu - \epsilon^\nu k^\mu) \,, \tag{A.4}$$

$$M_3 = -\gamma_5 \gamma_\mu q_\nu (\epsilon^\mu k^\nu - \epsilon^\nu k^\mu) \,, \tag{A.5}$$

$$M_4 = -\gamma_5 \gamma_\mu (p+p')_\nu (\epsilon^\mu k^\nu - \epsilon^\nu k^\mu) - 2M M_1 \,, \tag{A.6}$$

and the invariant amplitudes A_j for which one finds from (A.1)

$$A_1 = \frac{e\lambda}{m_\eta} \frac{g_t}{2M} \frac{t}{t - m_V^2} \,, \tag{A.7}$$

20

$$A_2 = -\frac{e\lambda}{m_\eta}\frac{g_t}{2M}\frac{1}{t-m_V^2}\,, \tag{A.8}$$

$$A_3 = 0\,, \tag{A.9}$$

$$A_4 = -\frac{e\lambda}{m_\eta}g_v\frac{1}{t-m_V^2}\,. \tag{A.10}$$

Introducing the operators $\tilde{M}_j$ in Pauli spinor space by $\chi_f^\dagger \tilde{M}_j \chi_i := \bar{u}_f M_j u_i$ and noting that $A_3 = 0$ for vector mesons, one finds for the remaining operators

$$\tilde{M}_1 = N'N\Big[-k_0\vec{\sigma}\cdot\vec{\varepsilon} - \frac{i\vec{\sigma}\cdot(\vec{k}\times\vec{\varepsilon})\,\vec{\sigma}\cdot\vec{p}}{e_p} + \frac{i\vec{\sigma}\cdot\vec{p}'\,\vec{\sigma}\cdot(\vec{k}\times\vec{\varepsilon})}{e_{p'}}$$
$$+\frac{k_0}{e_p e_{p'}}\vec{\sigma}\cdot\vec{p}'(\vec{p}\cdot\vec{\varepsilon} - i\vec{\sigma}\cdot(\vec{p}\times\vec{\varepsilon}))\Big]\,, \tag{A.11}$$

$$\tilde{M}_2 = N'N\Big[\frac{\vec{\sigma}\cdot\vec{p}'}{e_{p'}} - \frac{\vec{\sigma}\cdot\vec{p}}{e_p}\Big]\Big[J\vec{\varepsilon}\cdot(\vec{p}'+\vec{p}) - K\vec{\varepsilon}\cdot\vec{q}\Big]\,, \tag{A.12}$$

$$\tilde{M}_4 = N'N\Big[\Big(k_0\frac{\vec{\sigma}\cdot\vec{p}'}{e_{p'}} + k_0\frac{\vec{\sigma}\cdot\vec{p}}{e_p} - \vec{\sigma}\cdot\vec{k} - \vec{\sigma}\cdot\vec{p}'\,\vec{\sigma}\cdot\vec{k}\,\vec{\sigma}\cdot\vec{p}\frac{1}{e_p e_{p'}}\Big)$$
$$\times(\vec{p}\cdot\vec{\varepsilon}+\vec{p}'\cdot\vec{\varepsilon}) - \frac{K}{e_{p'}e_p}\vec{\sigma}\cdot\vec{p}'\,\vec{\sigma}\cdot\vec{\varepsilon}\,\vec{\sigma}\cdot\vec{p} - \vec{\sigma}\cdot\vec{\varepsilon}K\Big] - 2M\tilde{M}_1\,, \tag{A.13}$$

with $J = q\cdot k$, $K = (p+p')\cdot k$, $N^{(\prime)} = \sqrt{\frac{e_{p^{(\prime)}}}{2M}}$ and $e_{p^{(\prime)}} = E_{p^{(\prime)}} + M$.

We will now bring (A.2) into the form

$$i\tau_{fi} = \frac{e\lambda}{m_\eta}\frac{1}{t-m_V^2}\frac{N'N}{e_{p'}e_p}\chi_f^\dagger\Big(-g_v\tilde{M}_v + \frac{g_t}{2M}\tilde{M}_t\Big)\chi_i\,, \tag{A.14}$$

where we have introduced

$$\tilde{M}_v = \frac{e_{p'}e_p}{N'N}\tilde{M}_4\,, \tag{A.15}$$

$$\tilde{M}_t = \frac{e_{p'}e_p}{N'N}(t\tilde{M}_1 - \tilde{M}_2)\,. \tag{A.16}$$

In terms of the operators introduced in (40), we find explicitly

$$\tilde{M}_v = \frac{1}{4}\Big((s-u+4Mk_0)t + 2Me_-(m_\eta^2-t)\Big)\Omega^1 + (\frac{t}{2}+E_p e_+)\Omega^0_{\vec{k},\vec{p}'}$$
$$-(\frac{t}{2}+E_{p'}e_+)\Omega^0_{\vec{k},\vec{p}} + k_0 e_+\Omega^0_{\vec{p}',\vec{p}} + (\frac{t}{2}+Me_-)\Omega^2_{\vec{k},\vec{p}} + (\frac{t}{2}-Me_-)\Omega^2_{\vec{k},\vec{p}'}$$
$$+(k_0 M + \frac{1}{2}(s-M^2))(\Omega^2_{\vec{p}',\vec{p}'} - \Omega^2_{\vec{p},\vec{p}'}) + (k_0 M - \frac{1}{2}(u-M^2))(\Omega^2_{\vec{p},\vec{p}} - \Omega^2_{\vec{p}',\vec{p}})\,, \tag{A.17}$$

$$\tilde{M}_t = -\frac{t}{2}\Big(k_0 t + e_{p'}(s-M^2) - e_p(u-M^2)\Big)\Omega^1 + e_{p'}t\Big(\Omega^0_{\vec{k},\vec{p}} - \Omega^2_{\vec{k},\vec{p}}\Big)$$
$$-e_p t\Big(\Omega^0_{\vec{k},\vec{p}'} + \Omega^2_{\vec{k},\vec{p}'}\Big) - k_0 t\Omega^0_{\vec{p}',\vec{p}} - e_p(s-M^2)\Omega^2_{\vec{p}',\vec{p}'} + e_{p'}(u-M^2)\Omega^2_{\vec{p},\vec{p}}$$
$$+(k_0 t + e'\,(s-M^2))\Omega^2_{\vec{p},\vec{p}'} + (k_0 t - e\,(u-M^2))\Omega^2_{\vec{p}',\vec{p}}\,. \tag{A.18}$$

Here, s, t and u denote the usual Mandelstam variables and $e_{\pm} = e_{p'} \pm e_p$.

For the specialization to the γN c.m. sytem, we note the following relations using $\vec{p} = -\vec{k}$ and $\vec{p}' = -\vec{q}$

$$k_0 = \frac{1}{2W}(s - M^2)\,, \tag{A.19}$$

$$e_p = \frac{1}{2W}(W + M)^2\,, \tag{A.20}$$

$$e_{p'} = \frac{1}{2W}((W + M)^2 - m_\eta^2)\,, \tag{A.21}$$

with $W^2 = s$.

REFERENCES

[1] L. Tiator, C. Bennhold, S.S. Kamalov, G. Knöchlein, F.X. Lee, and L.E. Wright, Few-Body Syst., Suppl. 9 (1995) 213.

[2] C. Bennhold, L. Tiator, S.S. Kamalov, F.X. Lee, and L.E. Wright, πN-Newsletter 11 (1995) 78.

[3] Ch. Sauermann, B.L. Friman, and W. Nörenberg, πN-Newsletter 11 (1995) 147.

[4] M. Wilhelm, PhD thesis, Universität Bonn, 1993.

[5] B. Krusche *et al.*, Phys. Rev. Lett. 74 (1995) 3736.

[6] J.W. Price *et al.*, Phys. Rev. C 51 (1995) R2283.

[7] R.L. Anderson and R. Prepost, Phys. Rev. Lett. 23 (1969) 46.

[8] Yu. N. Kremenzova, A. I. Lebedev, AIP Conf. Proc. 1976, p. 634

[9] N. Hoshi, H. Hyuga, K. Kubodera, Nucl. Phys. A 342 (1979) 234.

[10] D. Halderson and A.S. Rosenthal, Nucl. Phys. A 501 (1989) 856.

[11] S.S. Kamalov, L. Tiator and C. Bennhold, preprint MKPH-T-95-22

[12] W. Beulertz, PhD thesis, Universität Bonn, 1994.

[13] B. Krusche *et al.*, Phys. Lett. B 358 (1995) 40.

[14] H.R. Hicks et al., Phys. Rev. D 7 (1973) 2614.

[15] C. Bennhold and H. Tanabe, Nucl. Phys. A 530 (1991) 625.

[16] M. Benmerrouche, N. Mukhopadhyay, and J. Zhang, Phys. Rev. D 51 (1995) 3237.

[17] G. Knöchlein, D. Drechsel, and L. Tiator, Z. Phys. A 352 (1995) 327.

[18] Ch. Sauermann, B.L. Friman, and W. Nörenberg, Phys. Lett. B 341 (1995) 261.

[19] Particle Data Group, *Review of Particle Properties*, Phys. Rev. D 50 (1994) 1173.

[20] Particle Data Group, *Review of Particle Properties*, Phys. Rev. D 45 (1992) 1.

[21] L. Tiator, C. Bennhold, and S.S. Kamalov, Nucl. Phys. A 580 (1994) 455.

[22] M. Kirchbach and L. Tiator, Nucl. Phys. A 604 (1996) 385.

[23] E. Breitmoser, diploma thesis, Universität Mainz, 1995.

[24] R. Machleidt, K. Holinde, and C. Elster, Phys. Rep. 149 (1987) 1.

[25] P. Wilhelm, and H. Arenhövel, Nucl. Phys. A 593 (1995) 435.

[26] S.S. Kamalov, private communication.

[27] P. Wilhelm, PhD thesis, Universität Mainz, 1992.

[28] G.F. Chew, M.L. Goldberger, F.E. Low, and Y. Nambu, Phys. Rev. 106 (1957) 1345.

TABLE I. Parameters for the vector mesons.

	m_V (MeV)	λ	λg_t	λg_v	Λ_V (MeV)
ρ	770	0.890	13.6085	2.2309	1800
ω	782	0.192	0	3.2640	1400

TABLE II. Resonance parameters giving the best agreement with the data.

$\Gamma^0_{S_{11}}$ (MeV)	$M_{S_{11}}$ (MeV)	$A^p_{1/2}$ (GeV$^{-\frac{1}{2}}$)	$g_{\eta N S_{11}}$	$g_{\pi N S_{11}}$
150	1535	$130 \cdot 10^{-3}$	2.033	1.148

TABLE III. Contribution of ω-meson to the t-matrix in the the γd c.m. system.

operator	$\tilde{M}_v$	$\tilde{M}_t$
Ω^1	$\frac{1}{4}\Big((s-u+4Mk_0)t + 2Me_-(m_\eta^2 - t)\Big)$	$-\frac{t}{4}\Big(2k_0 t + e_+(s-u) + e_-(m_\eta^2 - t)\Big)$
$\Omega^0_{\vec{k},\vec{q}}$	$-(\frac{t}{2} + p_0 e_+)$	$(p_0 + M)t$
$\Omega^2_{\vec{k},\vec{q}}$	$\frac{1}{2}(u - M^2 - m_\eta^2) + M(e_- - k_0)$	$(p_0 + M)t + e'(s - M^2)$
$\Omega^2_{\vec{q},\vec{q}}$	$\frac{1}{2}(s - M^2) + Mk_0$	$-e(s - M^2)$
$\Omega^0_{\vec{q},\vec{p}}$	$-k_0 e_+$	$k_0 t$
$\Omega^2_{\vec{q},\vec{p}}$	$\frac{1}{2}(t - m_\eta^2)$	$e\,m_\eta^2 - (k_0 + e)t$
$\Omega^0_{\vec{k},\vec{p}}$	$e_+(k_0 - e_-)$	$(e_- - k_0)t$
$\Omega^2_{\vec{k},\vec{p}}$	$\frac{1}{2}(t + m_\eta^2)$	$-\Big((p_0 + M)t + e'm_\eta^2\Big)$
$\Omega^2_{\vec{p},\vec{q}}$		$-\Big(k_0 t + e_-(s - M^2)\Big)$
$\Omega^2_{\vec{p},\vec{p}}$		$(2k_0 - e_-)t + e_- m_\eta^2$

TABLE IV. Contribution of ω-meson to the t-matrix in the γN c.m. system. The invariant mass is denoted by $W = W_{\gamma N}$ $(W^2 = s)$.

operator	$\tilde{M}_v$	$\tilde{M}_t$
Ω^1	$\frac{1}{4}\left((s - u + \frac{2M}{W}(s - M^2))t - \frac{m_\eta^2 M}{W}(m_\eta^2 - t)\right)$	$-\frac{t}{4W}\left(t(s - M^2) - \frac{1}{2}m_\eta^2(m_\eta^2 - t)\right.$ $\left.+((W + M)^2 - \frac{1}{2}m_\eta^2)(s - u)\right)$
$\Omega^0_{\vec{k},\vec{q}}$	$-\left(\frac{1}{2}(t - m_\eta^2) + (W + M)^2\right)$	$(W + M)t$
$\Omega^2_{\vec{k},\vec{q}}$	$\frac{1}{2}\left(u - M^2 - m_\eta^2 - \frac{M}{W}(s - M^2 - m_\eta^2)\right)$	$(W + M)t + \frac{1}{2W}((W + M)^2 - m_\eta^2)(s - M^2)$
$\Omega^2_{\vec{q},\vec{q}}$	$\frac{1}{2}(s - M^2)(1 + \frac{M}{W})$	$-\frac{(W+M)^2}{2W}(s - M^2)$

TABLE V. Various values for $A^n_{1/2}$, the ratio $A^n_{1/2}/A^p_{1/2}$ and the correlated values for $e\kappa^s_{S_{11}}$ and $A^s_{1/2}/A^p_{1/2}$ as used in this work. In addition, the last line shows the range of values that is found in the literature (see text).

	$A^n_{1/2}$ $[10^{-3}\text{GeV}^{-\frac{1}{2}}]$	$A^n_{1/2}/A^p_{1/2}$	$e\kappa^s_{S_{11}}$ $[10^{-3}\text{GeV}^{-\frac{1}{2}}]$	$A^s_{1/2}/A^p_{1/2}$
(A)	-106	-0.82	33.4	0.09
(B)	- 93	-0.72	51.0	0.14
(C)	- 82	-0.63	66.8	0.18
(D)	- 43	-0.33	120.6	0.33
(E)	-178	-1.37	- 66.8	-0.18
(F)	-217	-1.67	-120.6	-0.33
(G)	-29	-0.23	140.0	0.39
(Lit.)	-11 to -119	-0.65 to -1.5		-0.18 to +0.14
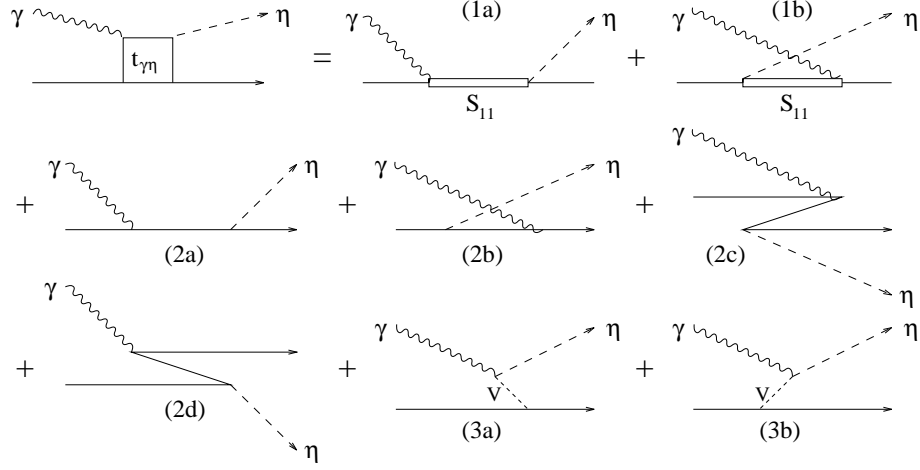
FIG. 1. Time ordered diagrams of all contributions: S_{11} resonance in s- (1a) and u-channel (1b), nucleon pole terms in s- (2a) and u-channel (2b) with z-graphs (2c) and (2d), and t-channel vector meson (V) exchange (3a) and (3b).
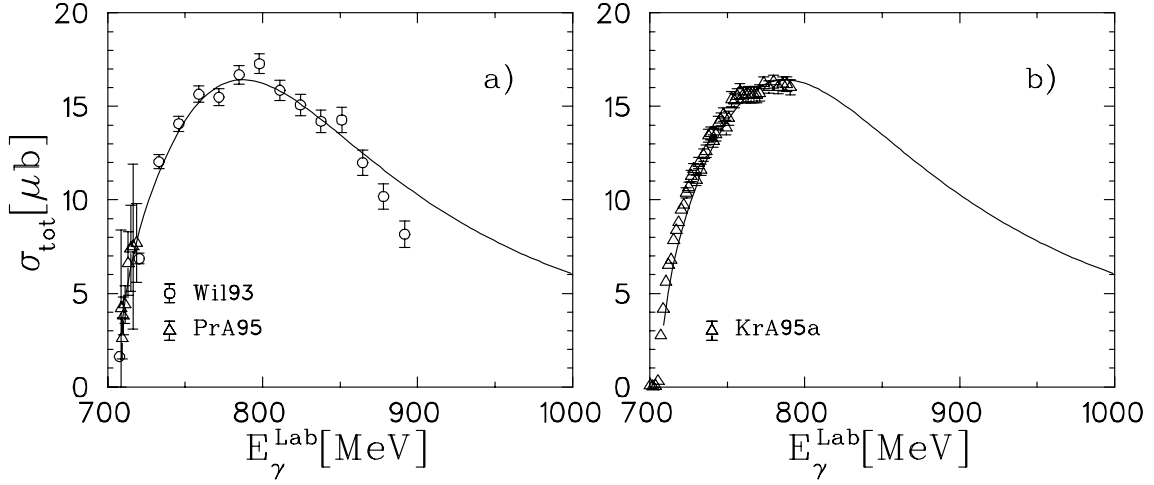

FIG. 2. Total cross section for $\gamma + p \to \eta + p$ using the parameters of Table II compared to the data of [4] and [6] (left) and [5] (right).
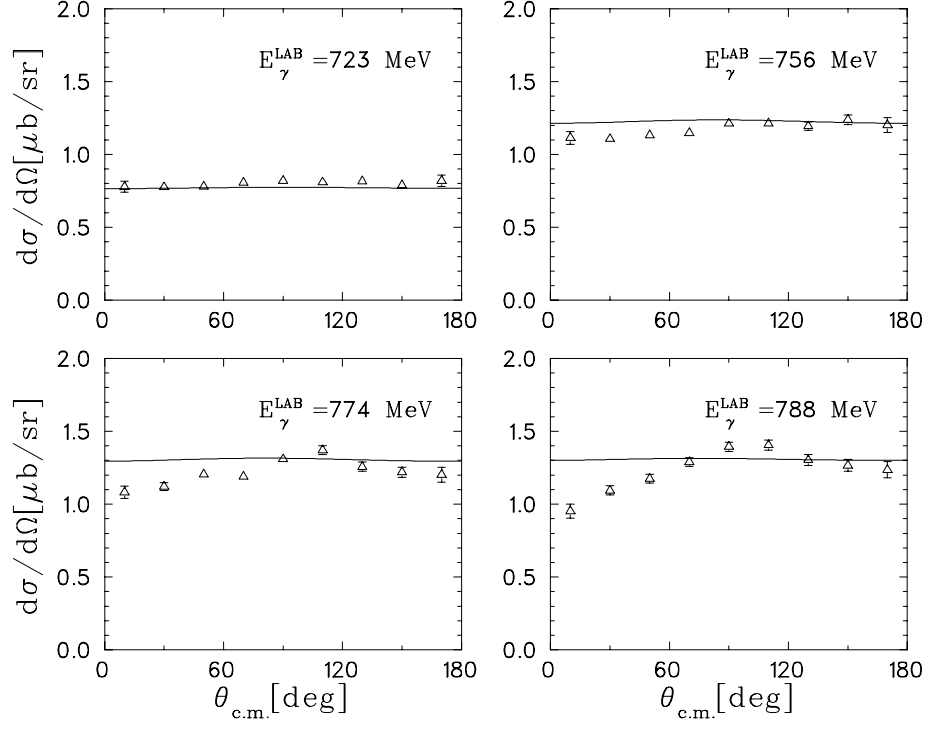
FIG. 3. Differential cross sections for $\gamma + p \to \eta + p$ for four photon energies using the parameters of Table II. Experimental data from [5].
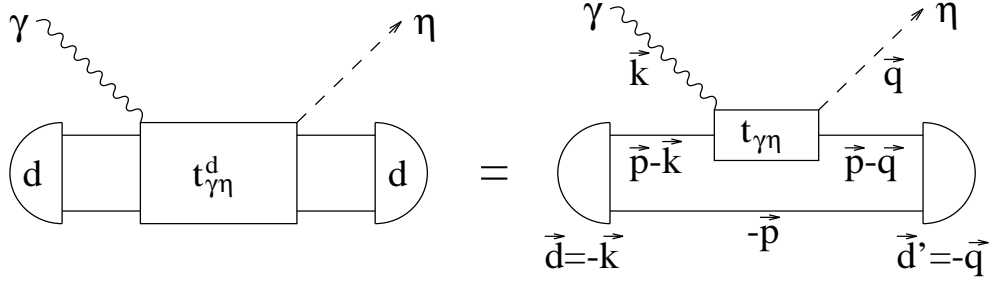
FIG. 4. Diagrammatic representation of $\gamma + d \to \eta + d$ in the impulse approximation with definition of momenta in the γd c.m. system.
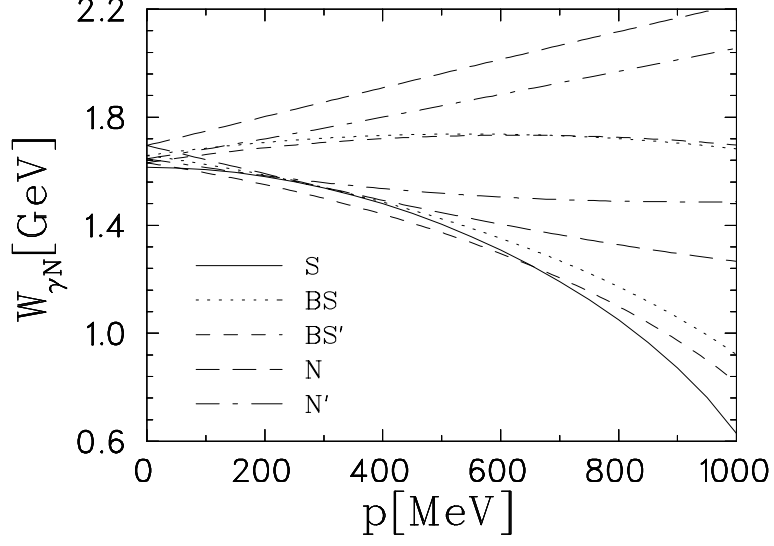
FIG. 5. The invariant mass $W_{\gamma N}$ of the active photon-nucleon subsystem as a function of the spectator momentum p. The energy is $E_\gamma^{Lab} = 800$ MeV, corresponding to $W_{\gamma d} = 2553$ MeV. The full curve shows $W_{\gamma N}^S$. For each of the other invariant mass assignments $W_{\gamma N}^{BS}$, $W_{\gamma N}^{BS'}$, $W_{\gamma N}^N$, and $W_{\gamma N}^{N'}$, two curves show the borderlines of the invariant mass region as explained in the inset.
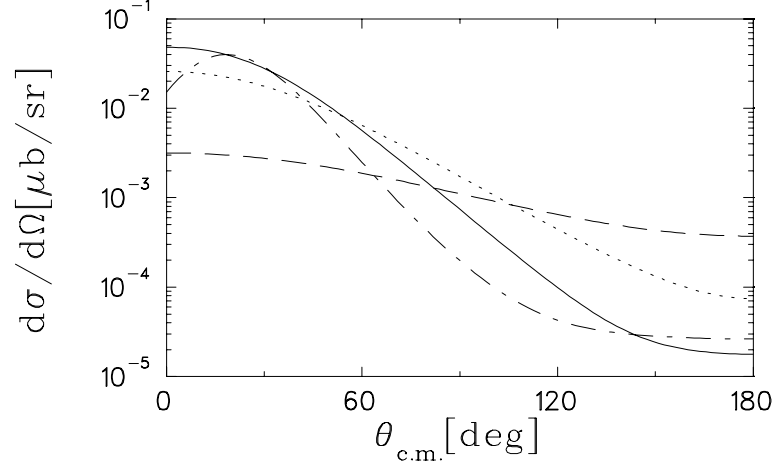
FIG. 6. Differential cross sections for various photon energies using $A_{1/2}^n = -106 \cdot 10^{-3} \text{GeV}^{-\frac{1}{2}}$: dashed curve for 640 MeV, dotted curve for 700 MeV, full curve for 800 MeV, and dashed-dotted curve for $E_\gamma^{Lab} = 1000$ MeV.
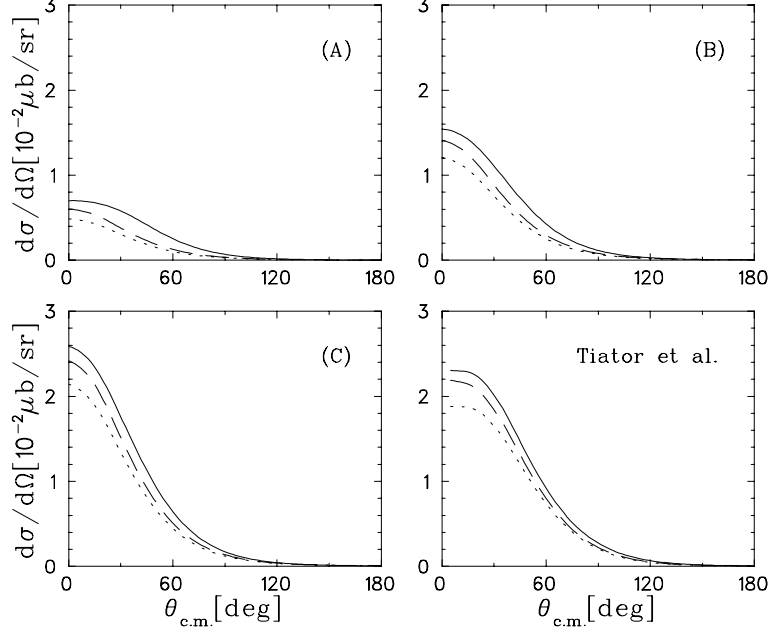
FIG. 7. Differential cross sections at $E_\gamma^{Lab} = 700$ MeV for different choices of the neutron S_{11} amplitude corresponding to the sets (A) to (C) of Table V. The lower right panel shows the result of [21]. The the dashed curves include only the resonance, the dotted ones the resonance and nucleon pole terms, and the full ones include all contributing graphs.
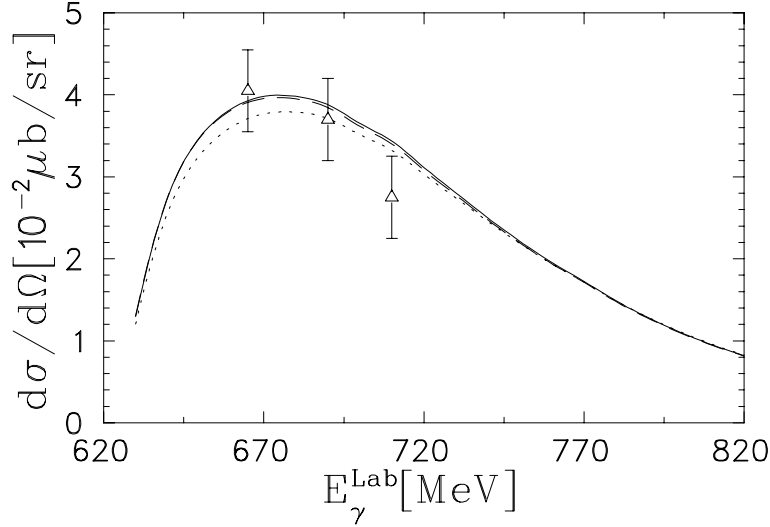

FIG. 8. Differential cross section at $\theta_{c.m.} = 90°$ as function of the photon lab energy. The notation of the curves as in Fig. 7. Here we have used $e\kappa^s = 340 \cdot 10^{-3} \text{GeV}^{-\frac{1}{2}}$. The data are taken from [7].

30
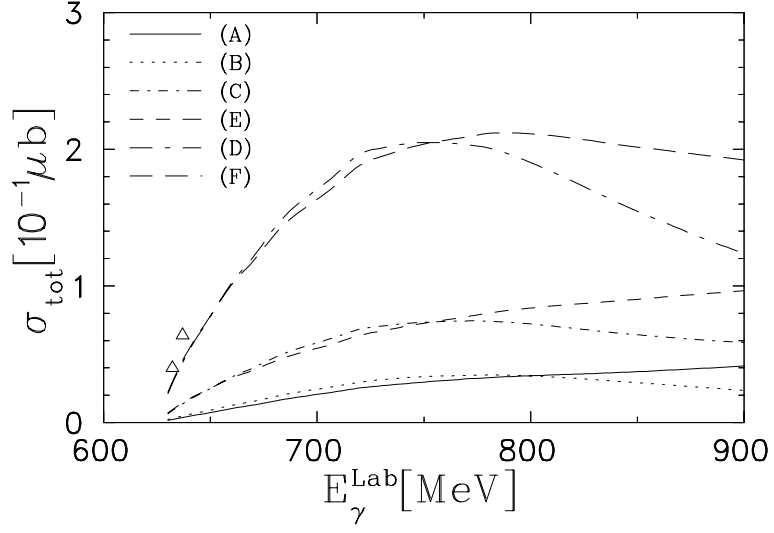
FIG. 9. Total cross section for the six different values of the neutron amplitude (A) - (G) of Tab. V. The triangles represent the upper limits of [12].
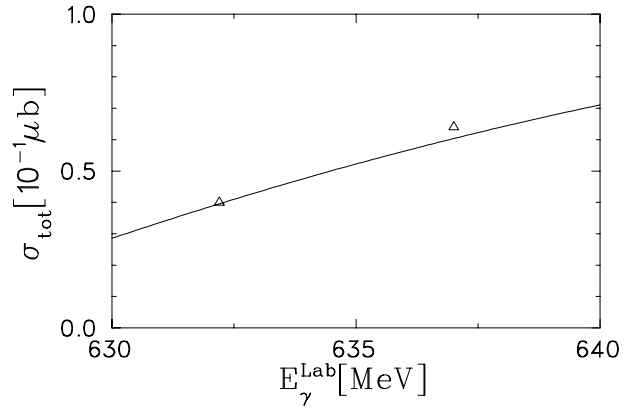

FIG. 10. Total cross section for a coupling constant $e\kappa^s_{S_{11}} = 140 \cdot 10^{-3} \mathrm{GeV}^{-\frac{1}{2}}$ (set (G) of Tab. V). The triangles represent the upper limits of [12].
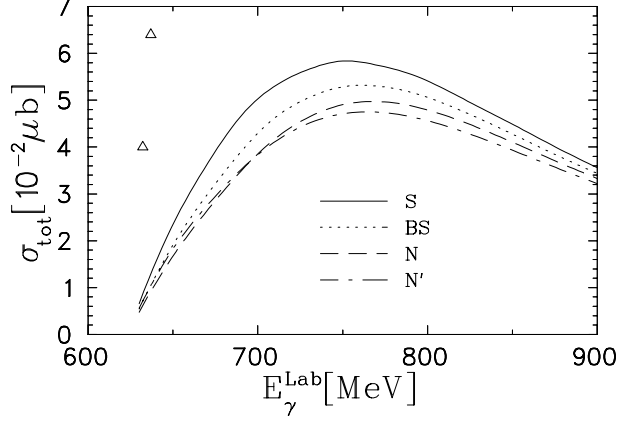
FIG. 11. Total cross section for the coherent reaction on the deuteron including only the resonance S_{11} for different choices of the invariant mass of the active subsystem using parameter set (C). The full curve with $W_{\gamma N}^{S}$, the dotted with $W_{\gamma N}^{BS}$, the dashed with $W_{\gamma N}^{N}$, and the dash-dotted with $W_{\gamma N}^{N'}$. The triangles represent the upper limit of [12].
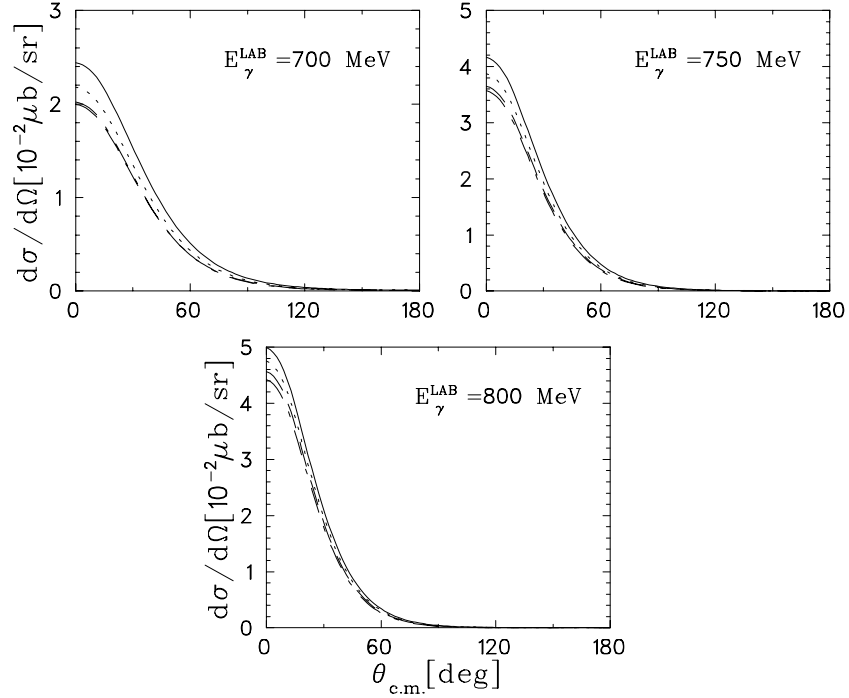

FIG. 12. Differential cross sections at three lab photon energies including only the resonance S_{11} for different choices of the invariant mass of the active subsystem using parameter set (C). The notation of the curves as in Fig. 11.
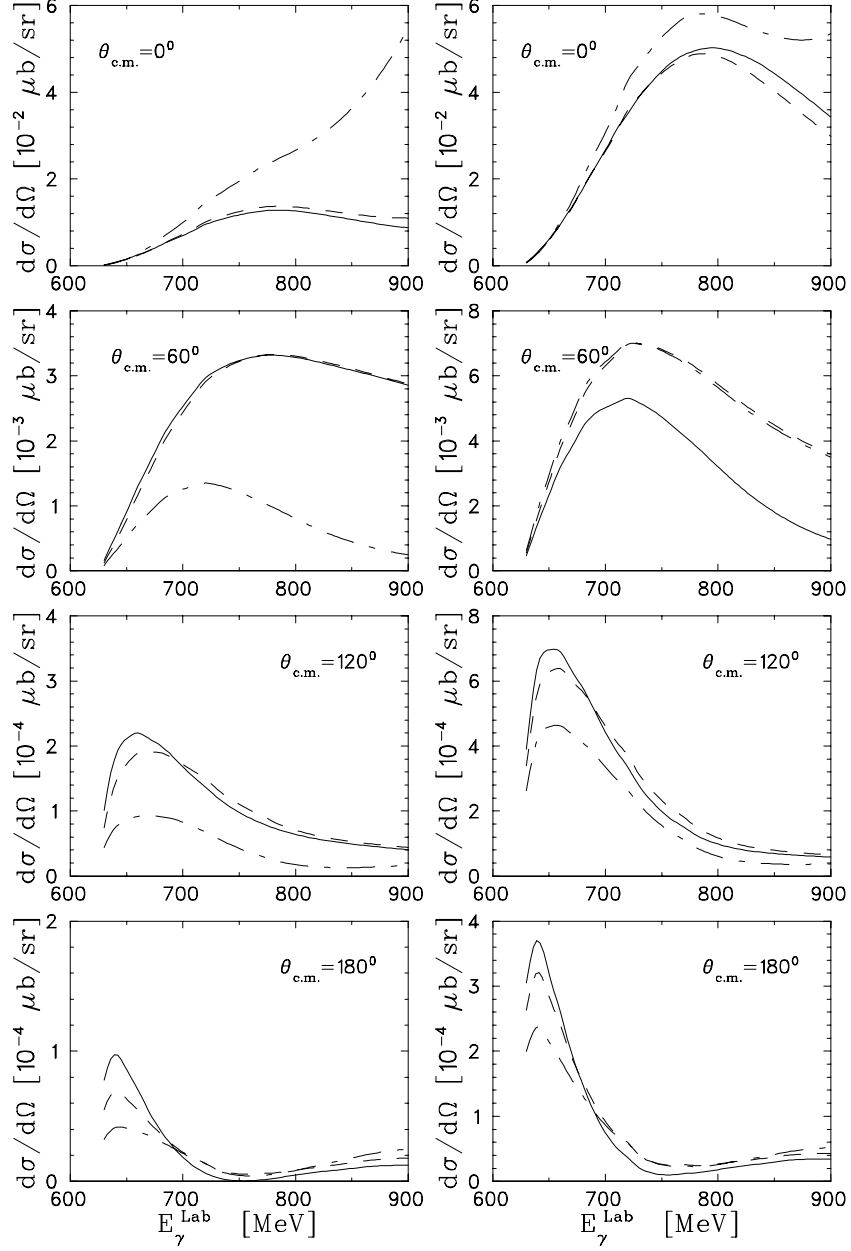
FIG. 13. Differential cross section as function of the photon lab energy for various constant angles, on the left side for parameter set (A) and on the right side for parameter set (C). The full curve shows the calculation using the general expression for ω exchange (GC), the dashed one is obtained with the Lorentz boosted operator for the ω meson contribution (LB) and for the dashed-dotted curves the c.m. elementary operator has been used without any transformation (CM).